A Singularity-Free Method for the Time-Dependent Schrödinger Equation for Nonlinear Molecules

A.D.Bandrauk[a,*], Hui-Zhong Lu[a]

[a]Labo. de Chimie Théorique, Faculté des Sciences, Université de Sherbrooke, Sherbrooke, PQ ,Canada J1K 2R1
{ andre.bandrauk, huizhong.lu}@usherbrooke.ca
[*] Canada Research Chair in Computational Chemistry and Photonics

We present a new method for the numerical solution of the Schrödinger equation using cylindrical/polar coordinates systems. For cylindrical coordinates systems, after use of a split-operator method which separates the z direction propagation and the (x, y) plane propagation, we approximate the wave function in each (x, y) section by a Fourier series ($\sum c_m(\rho)e^{im\phi}$) which offers an exponential convergence in the ϕ direction and is naturally applicable for polar coordinates system. The coefficients ($c_m(\rho)$) are then calculated by Finite Difference Method (FDM) in the ρ direction. We adopt the Crank-Nicholson method for the temporal propagation. The final linear system consists of a set of independent one-dimensional (ρ) linear systems and the matrix for every one-dimensional linear systems is sparse, so the whole linear system may be very efficiently solved. The most important advantage of the new method is that it is unitary at all steps and is analytically convergent every where even near the $\rho = 0$ origin, in contrast to most other numerical method based on cylindrical/polar coordinates systems which are not unitary and introduce a numerical singularity at $\rho = 0$. We also speculate on its generalization to the general case of dimension > 3 and the necessary computation power.

Nous présentons une nouvelles méthode de solution de l'équation de Schrödinger en coordonnées cylindriques ou polaires. En coordonnées cylindriques, après l'utilisation d'une opération qui sépare les propagations dans la direction z et dans le plan, nous appliquons une approximation de la fonction d'onde dans chaque section (x, y) par une série de Fourier ($\sum c_m(\rho)e^{im\phi}$) qui offre l'avantage d'une convergence exponentielle dans la direction ϕ et qui s'applique naturellement en coordonnées sphériques. Les coefficients ($c_m(\rho)$) sont ensuite calculés par la méthode des différences finies dans la direction ρ. Nous adoptons la méthode de Crank-Nicholson pour la propagation temporelle. Le système linéaire final est un ensemble de systèmes linéaires unidimensionnels (en ρ) et la matrice associée est creuse, donc le tout peut être résolue de manière efficace. Le principal avantage de la méthode est qu'elle est unitaire à chaque étape et converge analytiquement partout, même près de l'origine ($\rho = 0$), contrairement à la plupart des autres méthodes numériques basées sur les coordonnées cylindriques ou sphériques, qui ne sont pas unitaires et qui introduisent une singularité numérique à $\rho = 0$. Nous discutons de sa généralisation possible au cas de dimension > 3 et de la puissance de calcul requise.

1 Introduction

Because of efficiency, in many cases we use cylindrical coordinates for the numerical solution of the 3-D Time Dependent Schrödinger Equation, TDSE, for molecules exposed parallel to a intense laser pulse: H_2^+ [1–4], H_2 [5]. Generally, we use the split-operator method or the ADI method which separate the propagation in the different directions. This process reduces a lot of computing time and is very precise [6]. After splitting, we must propagate the wave function in each section plane in the polar coordinate. Polar coordinates have also been used in 2-D simulations of molecular alignment [3]. But in the polar coordinate system, one encounters often the (unitarity,precision) problem in the ρ direction when one uses Finite Difference Methods (FDM) and the difficulty of very expensive algorithms in CPU-time when one uses a development based on special functions such as Bessel function [1].

Because of its simplicity,the FDM is the most used in the ρ direction [1–4]. In order to avoid the boundary condition problem — there is no natural physical boundary condition at $\rho = 0$, one usually adopts the following nonlinear (stretching) transformation:

$$\rho = T(\tilde{\rho}), \tag{1}$$

$$\tilde{\psi}(\tilde{\rho}) = \sqrt{T'T}\psi(\rho), \tag{2}$$

$$\begin{aligned} i\frac{\partial\tilde{\psi}}{\partial t} &= -\frac{1}{2}\left[\frac{1}{T'^2}\frac{\partial^2}{\partial\tilde{\rho}^2} - 2\frac{T'''}{T'^3}\frac{\partial}{\partial\tilde{\rho}}\right]\tilde{\psi} \\ &+ \left[\frac{5}{4}\frac{T''^2}{T'^4} - \frac{1}{2}\frac{T'''}{T'^3} + \frac{1}{4T^2} + V\right]\tilde{\psi}, \end{aligned} \tag{3}$$

$$\tilde{\psi}(0) = 0, \qquad \tilde{\psi}(\tilde{\rho}_{max}) = 0, \tag{4}$$

The equation is restricted in the ρ direction after the use of the split-operator or ADI method in the polar coordinate (ρ, ϕ). Two problems (unitarity,convergence) occur as:
First:, when we discretize the differential operators in (3) with standart central difference schemes we find immediately the problem of unitarity: if $\rho/\tilde{\rho}$ is not constant, the resulting propagation matrix will not be symetrical, so the final discrete propagator is not unitary. This is just what occurs with transformations like $\rho = \tilde{\rho}^{3/2}$ (Kono and Kawata): $1/T' = 2/[3\sqrt{\tilde{\rho}}]$ shows that the coefficients of the second order derivative (kinetic energy) change very quickly near the origin so the propagation matrix is far from being symetrical near $\tilde{\rho} = 0$.
Second:, there is a problem of convergence which is very little discussed. It is well known that the convergence of

the FDM is based on the relation :

$$\begin{aligned}\tilde{\psi}(\tilde{\rho}+h) &= \sum_{i=0}^{n}\frac{h^i}{n!}\frac{d^i\tilde{\psi}}{d\tilde{\rho}^i}(\tilde{\rho}) \\ &+ \frac{h^n}{(n+1)!}\int_{\tilde{\rho}}^{\tilde{\rho}+h}\frac{d^{i+1}\tilde{\psi}(x)}{d\tilde{\rho}^{i+1}}dx, \quad (5)\end{aligned}$$

where the coefficient of the remaining term (integration) must be limited to obtain convergence. Now, after the transformation above we have $\rho=\tilde{\rho} \Longrightarrow \tilde{\psi}(\tilde{\rho})=\sqrt{\tilde{\rho}}\psi(\tilde{\rho})$, $\rho=\tilde{\rho}^{3/2} \Longrightarrow \tilde{\psi}(\tilde{\rho})=\sqrt{3/2}\tilde{\rho}\psi(\tilde{\rho}^{3/2})$. When $\psi(\rho)$ is an analytical function, we can make the development:

$$\begin{aligned}\frac{\partial^{i+1}\tilde{\psi}}{\partial\tilde{\rho}^{i+1}} &= \frac{\partial^{i+1}}{\partial\tilde{\rho}^{i+1}}\left[\sqrt{\tilde{\rho}}\psi(\tilde{\rho})\right] \\ &= \frac{\partial^{i+1}}{\partial\tilde{\rho}^{i+1}}\sum_{k=0}^{\infty}c_k\tilde{\rho}^{k+1/2} \\ &= \sum_{k=0}^{\infty}d_k\tilde{\rho}^{(2k-2i-1)/2} \text{ for } \rho=\tilde{\rho}, \quad (6)\end{aligned}$$

or

$$\begin{aligned}\frac{\partial^{i+1}\tilde{\psi}}{\partial\tilde{\rho}^{i+1}} &= \frac{\partial^{i+1}}{\partial\tilde{\rho}^{i+1}}\left[\sqrt{3/2}\tilde{\rho}\psi(\tilde{\rho}^{3/2})\right] \\ &= \frac{\partial^{i+1}}{\partial\tilde{\rho}^{i+1}}\sum_{k=0}^{\infty}c_k\tilde{\rho}^{1+3k/2} \\ &= \sum_{k=0}^{\infty}e_k\tilde{\rho}^{(3k-2i)/2} \text{ for } \rho=\tilde{\rho}^{3/2}. \quad (7)\end{aligned}$$

The two preceding equations show directly that with transformed wave function the integration term in (5) will not be finite (bounded) near $\tilde{\rho}=0$ for general cases. We also conclude that if $c_k=0$ for all k odd, equation (7) gives an analytical function so the equality (5) upon which the FDM's convergence is based is satisfied. This means that when $\psi(\rho)$ is an even function (*i.e* $\psi(\rho)=\psi(-\rho)$) the transformation $\rho=\tilde{\rho}^{3/2}$ will offer a convergent numerical scheme which is the special case of 2-D (ρ,ϕ) section non-passing by protons for 3-D H_2^+ exposed to a linearly polarize laser pulse which is parallel to the axis of the molecule [4] .

It is worth to note that when the wave function is independent of ϕ (eg. – molecule and laser parallel), some previous numerical methods (TaoZuo) have continued the function to the $\rho<0$ area by symmetry thus avoiding the boundary condition problem at $\rho=0$. Even without the preceding singular transformation, the original differential operator $\frac{\partial^2}{\partial\rho^2}+\frac{1}{\rho}\frac{\partial}{\partial\rho}$ is not in self-adjoint form, so the discrete propagator is still non-unitary. Another weakness of this method of propagation is that it is not available for wave functions which are dependent on ϕ as is the case for the one-electron H_2^+ in a perpendicular laser field or for the two-electrons H_2 exposed to a general laser pulse.

The consequence of the above two problems is that the non-unitarity may make the numerical method unstable and the non-analytic behaviour of the transformed wavefunction near the origin make the method very poor in precision. For the continuation to $\rho<0$ method (TaoZuo), we have found that: for H_2^+ parallel to a linear laser pulse, after preparation of the initial condition by an imaginary time step method, and coming back to real time with zero laser intensity, the population diminishes to 95% because of the non-unitarity of the discretized operator.

To overcome the preceding difficulties of FDM in the ρ direction, our idea is to first write the operator $\frac{\partial^2}{\partial\rho^2}+\frac{1}{\rho}\frac{\partial}{\partial\rho}$ in self-adjoint form — $\frac{1}{\rho}\frac{\partial}{\partial\rho}\rho\frac{\partial}{\partial\rho}$ which help us to obtain a unitary discrete operator (for detail, see next section). To avoid the problem of boundary conditions at $\rho=0$, we propagate the wave function in the whole plane without separating ρ and ϕ so we do not use the above wave function transformations which cause problems of convergence.

We must emphasise that the separation $(1+c\frac{\partial^2}{\partial\rho^2}+c\frac{1}{\rho}\frac{\partial}{\partial\rho})(1+c\frac{1}{\rho^2}\frac{\partial^2}{\partial\phi^2}) = 1+c(\frac{\partial^2}{\partial x^2}+\frac{\partial^2}{\partial y^2})+c^2(\frac{\partial^2}{\partial\rho^2}+c\frac{\partial}{\partial\rho}/\rho)(\frac{\partial^2}{\partial\phi^2}/\rho^2)$ results that the error term (3rd term of this equality) is very difficult to be limited in numerical simulation and this is just the error term appearing in the split-operator method which separates ρ and ϕ direction propagation. We will demonstrate the advantage of our choice to propagate the wave function in the whole plane without separating ρ and ϕ.

2 The numerical method

As explained in the preceding section, after using the splitting method in 3-D which separates the z-coordinate, the main numerical difficulty comes from the free propagation of the wave function in the remaining 2-D plane in polar coordinates (ρ,ϕ).

For details for the splitting method we refer to [6], and we concentrate here on studing the approximation of the free propagation equation in 2-D:

$$i\frac{\partial F}{\partial t}=-\alpha\left[\frac{\partial^2}{\partial\rho^2}+\frac{1}{\rho}\frac{\partial}{\partial\rho}+\frac{1}{\rho^2}\frac{\partial^2}{\partial\phi^2}\right]F. \quad (8)$$

We adopt the Crank-Nicholson method for the temporal approximation of (8):

$$\begin{aligned}&\left\{1-i\frac{\delta t}{2}\alpha\left[\frac{1}{\rho}\frac{\partial}{\partial\rho}\rho\frac{\partial}{\partial\rho}+\frac{1}{\rho^2}\frac{\partial^2}{\partial\phi^2}\right]\right\}F(\rho,\phi,t_{l+1}) \\ =\; &\left\{1+i\frac{\delta t}{2}\alpha\left[\frac{1}{\rho}\frac{\partial}{\partial\rho}\rho\frac{\partial}{\partial\rho}+\frac{1}{\rho^2}\frac{\partial^2}{\partial\phi^2}\right]\right\}F(\rho,\phi,t_l). \quad (9)\end{aligned}$$

For the spatial approximation of (9), we use the truncated Fourier series,

$$\begin{aligned}&F(\rho,\phi,t_l) \\ =\; &\frac{1}{N}\sum_{n=0}^{N-1}c_n^l(\rho)e^{in\phi} \quad (10) \\ =\; &\frac{1}{N}\left[\sum_{n=0}^{N/2-1}c_n^l(\rho)e^{in\phi}+\sum_{n=N/2}^{N-1}c_n^l(\rho)e^{i(n-N)\phi}\right],\end{aligned}$$

where $\{c_n(\rho)\}$ is the unknown set of functions on ρ. The preceding formula shows that for fixed ρ, $\{c^l_n(\rho)\}_{n=0}^{N-1}$ is just the discrete Fourier coefficients of $F(\rho,\phi,t_l)$ as a function of ϕ. So we have:

$$\begin{aligned} c^l_n(\rho) &= \sum_{m=0}^{N-1} F(\rho,\frac{m}{N}2\pi,t_l)e^{-in2\pi m/N} \\ &\qquad \text{for n=0,N-1,} \qquad (11)\\ &\equiv \sum_{m=0}^{N-1} F(\rho,\frac{m}{N}2\pi,t_l)e^{-i(n-N)2\pi m/N} \\ &\qquad \text{for n=N/2,N-1.} \end{aligned}$$

For a regular function F, we can demonstrate that $c_{n\neq 0}(\rho=0)$ should be zero by developping the function in the series:

$$F(\rho,\phi)=\sum_{i,j} a_{i,j}x^iy^j. \qquad (12)$$

At $\rho=0$, only the $a_{0,0}$ term of the series contributes to the integration in (11), but for $n\neq 0$ we have $\int a_{0,0}e^{in\phi}d\phi=0$. It should be noted that the $c_{n\neq 0}(\rho=0)=0$ condition insures also that the function in the series (10) is well defined at the origin ($\rho=0$). To study the coefficient $c_0(\rho)$, we first rewrite it from (11) as:

$$\begin{aligned} c_0(\rho) &= \sum_{m=0}^{N-1} F(\rho,\frac{m}{N}2\pi)=\frac{N}{2\pi}\int_0^{2\pi}F(\rho,\phi)d\phi \\ &= \frac{N}{2\pi}\sum a_{j,k}\int_0^{2\pi}x^jy^kd\phi. \qquad (13) \end{aligned}$$

For $j+k$ even, the integral $\int_0^{2\pi}x^jy^kd\phi$ will be zero because of the anti-symmetry. So we have :

$$c_0(\rho)=\frac{N}{2\pi}\sum_{j+k\in 2\aleph} a_{j,k}\int_0^{2\pi}x^jy^kd\phi=\sum_m b_{2m}\rho^{2m}. \quad (14)$$

More precisely, for regular function F, we have:

$$\begin{aligned} c_{2n}(\rho) &= \sum_{2m\geq 2n} a_{2m}\rho^{2m} \\ &\qquad \text{for } 0\leq 2n<N/2,\\ c_{2n+1}(\rho) &= \sum_{2m+1\geq 2n+1} a_{2m+1m}\rho^{2m+1} \\ &\qquad \text{for } 0\leq 2n+1<N/2,\\ c_{2n}(\rho) &= \sum_{2m\geq(N-2n)} a_{2m}\rho^{2m} \qquad (15)\\ &\qquad \text{for } N/2\leq 2n\leq N-1,\\ c_{2n+1}(\rho) &= \sum_{2m+1\geq(N-2n-1)} a_{2m+1m}\rho^{2m+1} \\ &\qquad \text{for } N/2\leq 2n+1\leq N-1. \end{aligned}$$

This permits us to use higher order finite difference schemes as accurate as necessary.

Now using (10) in (9), we get:

$$\begin{aligned} &\sum_{n=0}^{N/2-1}\left[1-i\frac{\delta t}{2}\alpha D_{\rho,\,n}\right]c_n^{l+1}e^{in\phi} \\ +&\sum_{n=N/2}^{N-1}\left[1-i\frac{\delta t}{2}\alpha D_{\rho,\,n}\right]c_n^{l+1}e^{i(n-N)\phi} \\ =&\sum_{n=0}^{N/2-1}\left[1-i\frac{\delta t}{2}\alpha D_{\rho,\,n}\right]c_n^{l}e^{in\phi} \\ +&\sum_{n=N/2}^{N-1}\left[1-i\frac{\delta t}{2}\alpha D_{\rho,\,n}\right]c_n^{l}e^{i(n-N)\phi}, \qquad (16) \end{aligned}$$

with the differential operator:

$$\begin{aligned} D\rho,\,n &= \frac{1}{\rho}\frac{\partial}{\partial\rho}\rho\frac{\partial}{\partial\rho}-\frac{n^2}{\rho^2} \text{ for } 0\leq n<N/2 \qquad (17)\\ &= \frac{1}{\rho}\frac{\partial}{\partial\rho}\rho\frac{\partial}{\partial\rho}-\frac{(n-N)^2}{\rho^2} \text{ for } N/2\leq n<N. \end{aligned}$$

So we get the following set of ODE's for $c_n^{l+1}(\rho)$:

$$\left[1-i\frac{\delta t}{2}\alpha D_{\rho,\,n}\right]c_0^{l+1}=\left[1+i\frac{\delta t}{2}\alpha D_{\rho,\,n}\right]c_0^{l} \qquad (18)$$

for $0\leq n<N$.

We adopt the following second order FDM to approximate $c_n(\rho)$ of (18) at a set of grid points — $\{\rho_m, m\geq 0\}$ with $\rho_0=0$:

$$\begin{aligned} \frac{1}{\rho}\frac{\partial}{\partial\rho}\rho\frac{\partial}{\partial\rho}c_n(\rho_m) &= \rho_{m+1/2}c_n(\rho_{m+1})/\rho_mh^2 \qquad (19)\\ &- (\rho_{m+1/2}+\rho_{m-1/2})c_n(\rho_m)/\rho_mh^2 \\ &+ \rho_{m-1/2}c_n(\rho_{m-1})/\rho_mh^2+\mathcal{O}(h^2) \end{aligned}$$

where h is the uniform spatial step. We need to fix the boundary condition here:

1. at $\rho=\rho_{max}$, we use the zero Dirichlet condition as usual;

2. at $\rho=0=\rho_0$:
   for $c_{n\neq 0}$, we have demonstrated in the preceding section that $c_{n\neq 0}(\rho=0)=0$;
   for c_0, we have no explicit boundary condition, but we can use

   $$\frac{1}{\rho}\frac{\partial}{\partial\rho}\rho\frac{\partial}{\partial\rho}c_0(\rho=0)=4\frac{c_0(h)-c_0(0)}{h^2}+\mathcal{O}(h^2) \quad (20)$$

   which can easily be shown by using (14).

Finally, it is not difficult to show that the resulting propagation matrix is *always symetric* with respect to the discrete L_2 scalar product: $<F,G>=\frac{\pi\rho_1^2}{4}F(\rho=0)G^*(\rho=0)+\sum_{n=0\ldots N-1,m=1..M}\frac{2\pi}{N}hF(\rho_m,\phi_n)G^*(\rho_m,\phi_n)$. The important consequence is that the propagator will be always unitary.

3 Numerical results

First, we have implemented four numerical methods to compare their convergence and unitarity when applied to the 2-D Schrödinger equation in polar coordinates:

1. The splitting method with FFT in xy – Cartesian coordinate (denoted SPLIT-xFFT-yFFT);
2. The splitting method with FFT in ϕ and FD in ρ – polar coordinate (denoted SPLIT-ρDF-ϕFFT-1) where the wave function is transformed by (2) with $\bar{\rho} = \rho$. In this transformation, the first derivative is eliminated but a new singular potential, $1/4T^2 = 1/4\rho^2$ is added (equation (3));
3. The splitting method with FFT in ϕ and FD in ρ – polar coordinate (denoted SPLIT-ρDF-ϕFFT-2) where the wave function is transformed by (2) with $\rho = \bar{\rho}^{3/2}$. In this transformation, in adition to the singular potential added, the transformed wavefunction becomes a singular function at origin;
4. The present method without splitting of ρ and ϕ (denoted GLOBAL-ρDF-ϕFFT).

3.1 Unitarity of the 3 methods in polar coordinate

In order to test the unitarity, we have initialized the wave function with $\psi(k*h, \phi) = (k*h)*(-1)^k*(1+e^{i\phi}+e^{i\phi*N/2})$ which is very singular but every unitary discrete propagator should conserve it's norm. The discrete propagators are obtained with the three methods in polar coordinates for H_3^{++} in 2-D and a laser pulse of intensity $I = 10^{14}W/cm^2$ and $\lambda = 800nm$. In Fig 1, we compare the evolution of the total population without absorber near boundaries for all three methods: SPLIT-ρDF-ϕFFT-1,SPLIT-ρDF-ϕFFT-2,GLOBAL-ρDF-ϕFFT. We can't distinguish the curves for SPLIT-ρDF-ϕFFT-1 and GLOBAL-ρDF-ϕFFT, but we see a clear fluctuation for the result of SPLIT-ρDF-ϕFFT-2 which demonstrates the non-unitarity of this method of transformation.

3.2 Problem of numerical sigularity

To illustrate the precision of the three different methods in polar coordinates, we have solved numerically the 2-D Schrödinger equation for H_3^{++} exposed to a linearly polarized (in x axis direction) laser field: intensity $I = 10^{14}W/cm^2$, wavelength $\lambda = 800nm$. The 3 protons' position are shown in Fig 2 with $R = 6$, $\theta = 60^o$ and $\alpha = 0^o$. It's well known that the convergence on the phase of the wave function is much more difficult to obtain than it's absolute value [6] .

Here, the converged solution has been obtained by SPLIT-xFFT-yFFT and we show the numerical results for the 3 methods in polar coordinates for the real (R) and imaginary (Im) parts in Fig 4 for $t = 1$ and 5 cycles. We see that the two methods of nonlinear transformation ($\rho = \tilde{\rho}$ and $\rho = \tilde{\rho}^{3/2}$) have introduced numerical sigularities at the origin. In contrast, the present method does not introduce any numerical singularity at $\rho = 0$ and gives very good convergence. It's to be noted that all three methods in polar coordinates have used the same number of discretization points in each direction (ρ,ϕ). As illustration, we show also the population contour for $t = 5$ cycles in Fig 5 for all four methods which confirm again that the SPLIT-ρDF-ϕFFT-1 method has not yet converged to the exact solution. The SPLIT-ρDF-ϕFFT-2 method performs well away from the singularity.

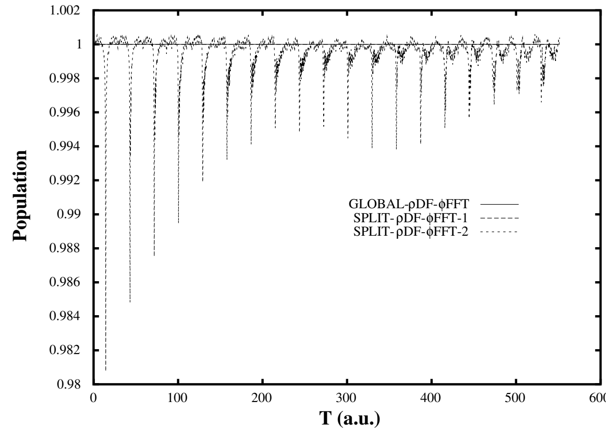

Figure 1. Evolution of the total population for 3 methods in polar coordinates

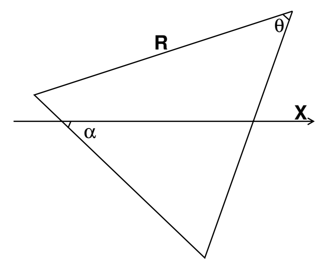

Figure 2. The protons' position for H_3^{++}

3.3 New numerical results with circularly polarized laser field

Finally, we show some numerical results for H_3^{++} with different configurations exposed to a circularly polarized laser field: intensity $I = 2 \times 10^{14}W/cm^2$, wavelength $\lambda = 800nm$. We have calculated the ionization for different combination of R and θ: $(R, \theta) = (4+0.25*k, j*7.5^o)$ for $0 \le k \le 24$ et $1 \le j \le 24$. In Fig 3, we show the contour of the ionized population as function of (R, θ) at $t = 10$ cycles. In Fig 6, we show the population contour for some special configuration at $t = 10$ cycles where the ionization is maximum.

4 Conclusion

We have developped a new numerical method for the numerical solution of the Time-Dependent Schrödinger Equation in polar (2-D) / cylindrical (3-D) coordinates. Our numerical results have demonstrated the advantage of the present method compared to other methods in these coordinates: unitarity of the discrete propagator, and no numerical singularity. This method will be extended to solve the problem of two electron interaction in H_3^+ with a laser field in 2-D: we first map the processors on a 2-D Cartesian grid, then the data will be distributed through the 2-D grid along the (ρ_1, ρ_2) direction; with this distribution the FFT transformation will be local in each processor and the solution of the 1-D discrete linear system obtained with splittin method in (ρ_1, ρ_2) or the 2-D discrete system without splitting will be worked out in parallel. Later, this method can be easily extended to H_3^+ with nuclear R variable – leading to a 5 variable $(R, \rho_1, \theta_1, \rho_2, \theta_2)$ problem.

References

1. S. Chelkowski, T. Zuo, A.D. Bandrauk, "Ionization Rates of H_+^2 in an Intense Laser Field by Numerical Integration of the Time-dependent Schrödinger Equation", Phys. Rev. **A46**, R5342 (1992).
2. T. Zuo, A.D. Bandrauk, M. Ivanov, P.B. Corkum, "Control of High-order Harmonic Generation in Strong Laser Fields", Phys. Rev. **A51**, 3991 (1995).
3. C. Dion, "Simulation Numérique de l'Isomérisation de HCN en Champ Laser Intense", (Mémoire de maîtrise en sciences, 1995).
4. H. Kono, A. Kita, Y. Ohtsuki, Y. Fujimura, "An Efficient Quantum Mechanical Method for the Electronic Dynamics of the Three-dimensional Hydrogen Atom Interacting with a Linearly Polarized Strong Laser Pulse", J. Comp. Phys. **130**, 148 (1997).
5. K. Harumiya, H. Kono, Y. Fujimura, I. Kawata, A.D. Bandrauk, "Intense Laser-field Ionization of H_2 Enhanced by Two-electron Dynamics" Phys. Rev. **A66**, 043403 (2002).
6. A.D. Bandrauk, H. Shen, "Exponential Split Operator Methods for Solving Coupled Time-dependent Schrodinger Equations", J. Chem. Phys. **99**, 1185 (1993).

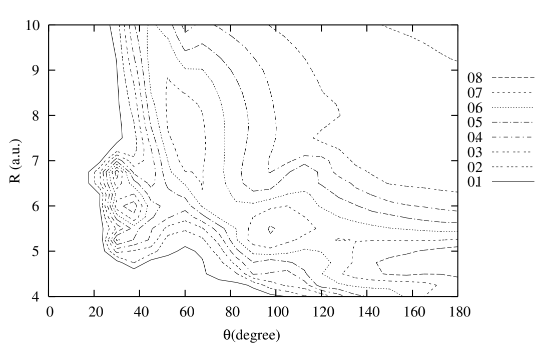

Figure 3. Ionization of H_3^{++} exposed to circularly polarized laser filed in different (R, θ) configuration

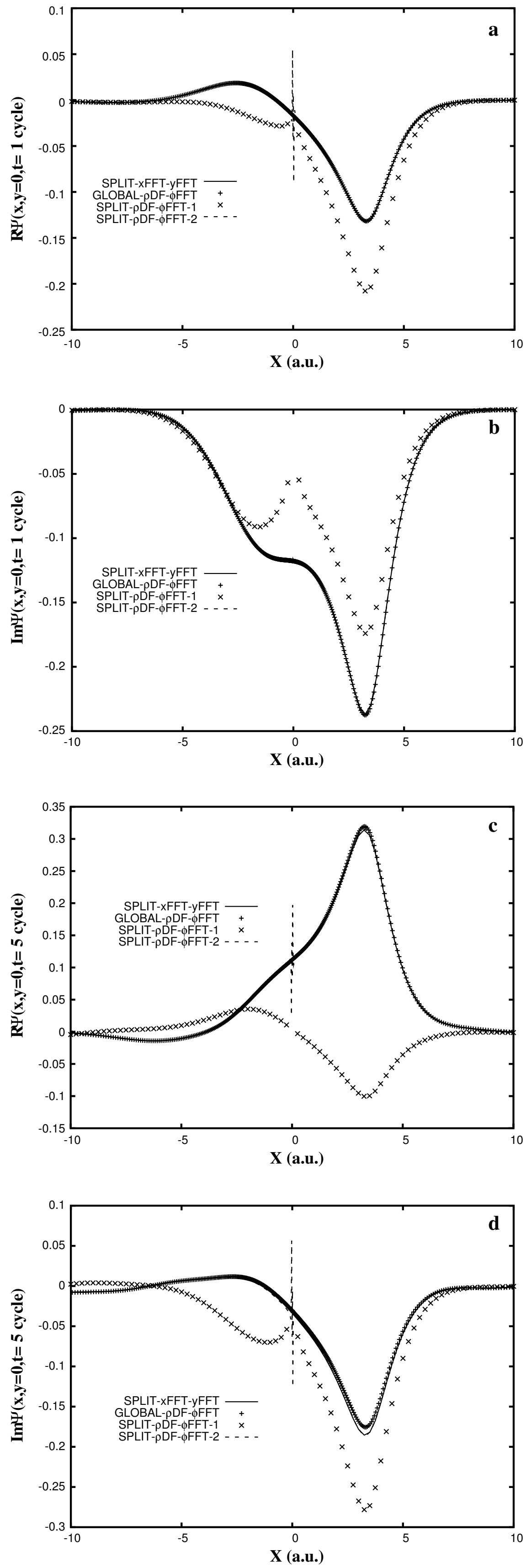

Figure 4. Numerical singularity

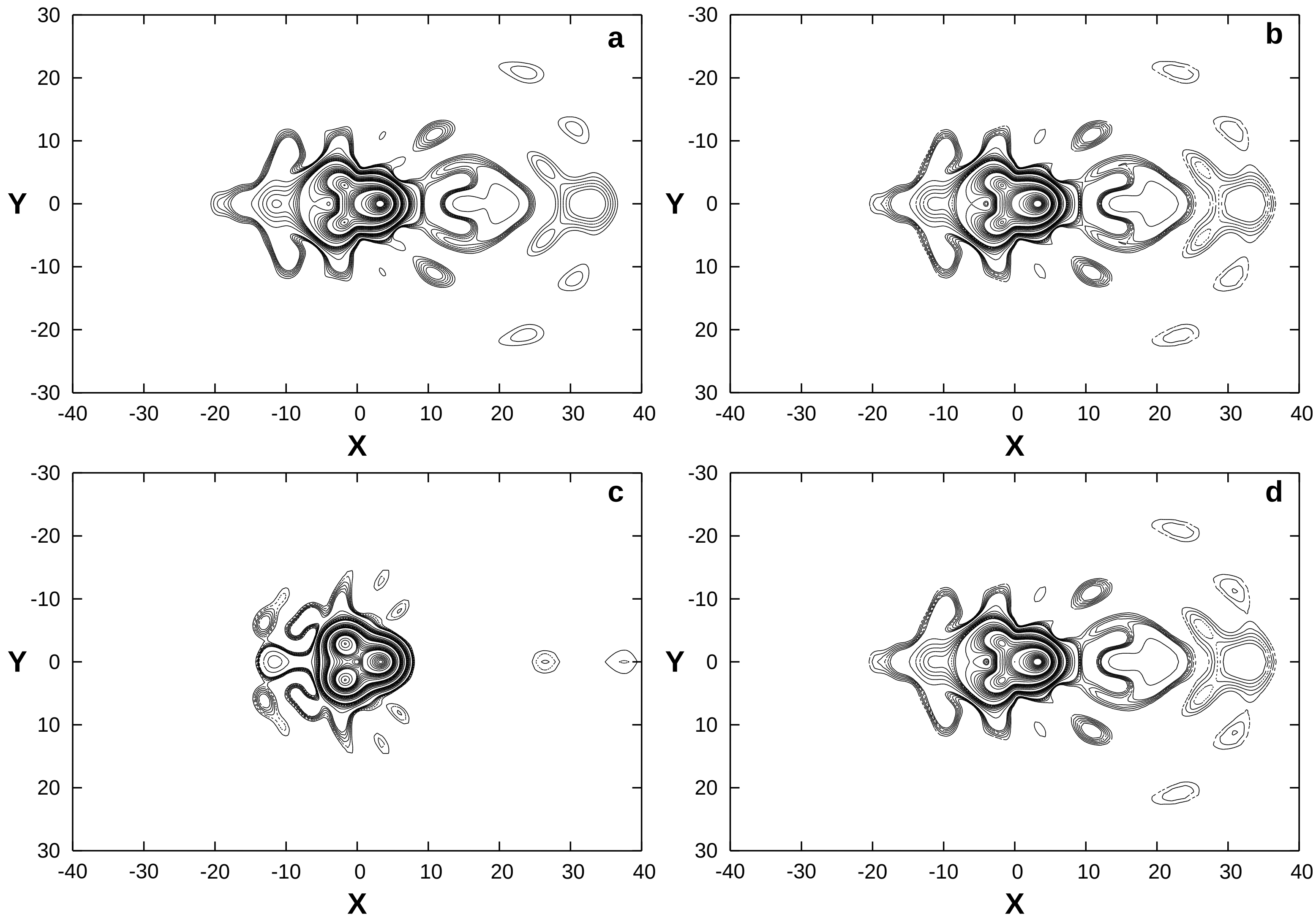

Figure 5. Population iso-line contour: a — SPLIT-xFFT-yFFT, b — GLOBAL-ρDF-ϕFFT, c — SPLIT-ρDF-ϕFFT-1, d — SPLIT-ρDF-ϕFFT-2

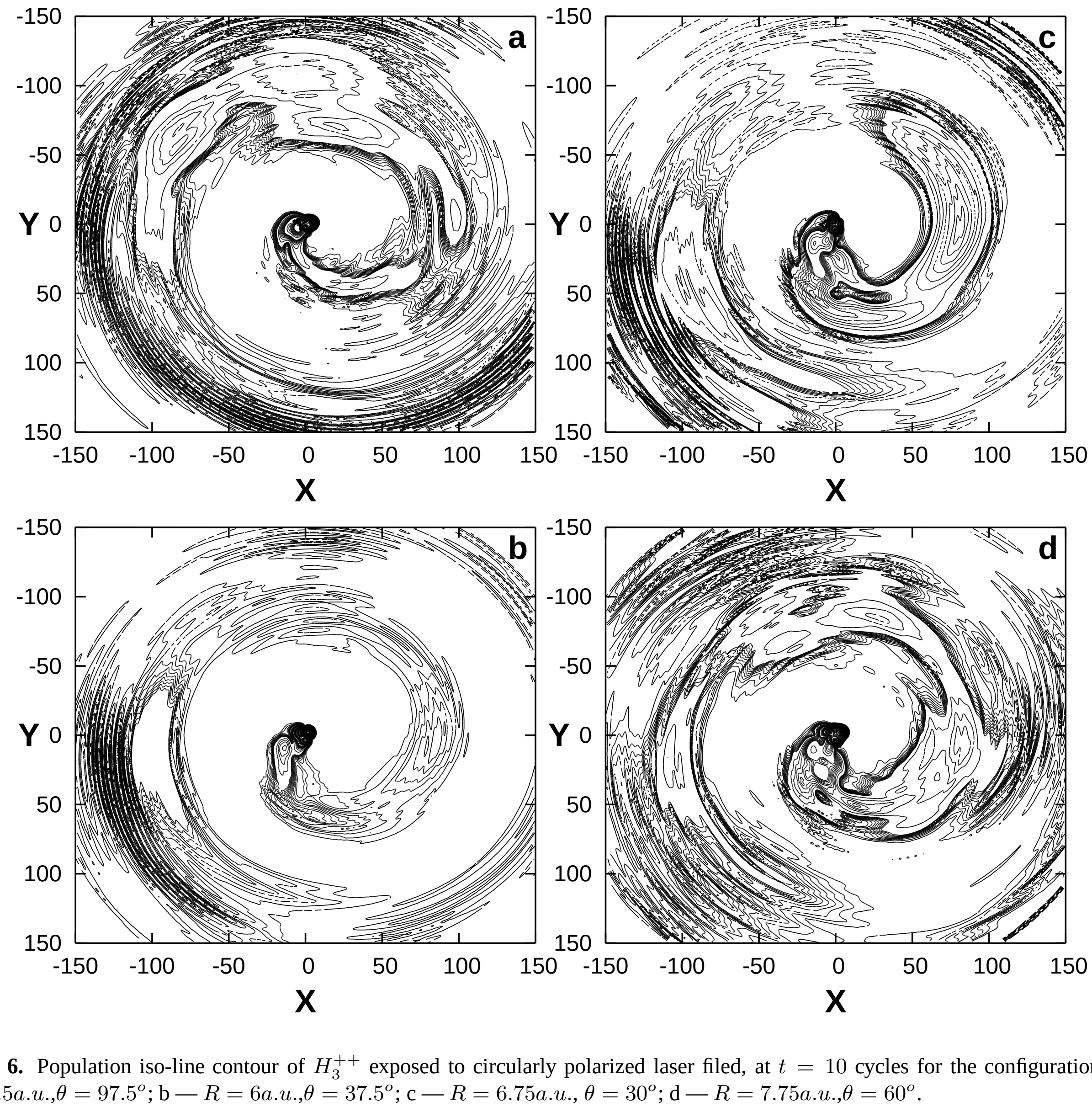

Figure 6. Population iso-line contour of H_3^{++} exposed to circularly polarized laser filed, at $t = 10$ cycles for the configurations: a — $R = 5.5a.u.$,$\theta = 97.5^o$; b — $R = 6a.u.$,$\theta = 37.5^o$; c — $R = 6.75a.u.$, $\theta = 30^o$; d — $R = 7.75a.u.$,$\theta = 60^o$.